DOI: 10.1021/ma100767b

Macromolecules
ARTICLE

Synthesis and Photovoltaic Properties of Bithiazole-Based Donor−Acceptor Copolymers

Maojie Zhang,[†,‡] Haijun Fan,[†,‡] Xia Guo,[†] Youjun He,[†] Zhiguo Zhang,[†] Jie Min,[†] Jing Zhang,[†,‡] Guangjin Zhao,[†] Xiaowei Zhan,*[,†] and Yongfang Li*[,†]

[†]*Beijing National Laboratory for Molecular Sciences, CAS Key Laboratory of Organic Solids, Institute of Chemistry, Chinese Academy of Sciences, Beijing 100190, China, and* [‡]*Graduate University of Chinese Academy of Sciences, Beijing 100039, China*

Received April 9, 2010; Revised Manuscript Received June 4, 2010

ABSTRACT: Three new donor−acceptor (D−A) alternative copolymers containing bithiazole acceptor unit and the donor unit of carbazole (**P1**), dithienopyrrole (**P2**), or dithienosilole (**P3**) were synthesized for the application as donor materials in polymer solar cells (PSCs). The copolymers were characterized by TGA, UV−vis absorption, electrochemical cyclic voltammetry and photovoltaic measurements. The results indicate that the donor units in the copolymers influence the bandgaps, electronic energy levels and photovoltaic properties of the copolymers significantly. Among the three copolymers, **P3** with the donor unit of dithienosilole shows an absorption spectrum similar to that of P3HT, suitable HOMO energy level at −5.18 eV, a higher hole mobility of 3.07×10^{-4} cm^2/V s and promising photovoltaic properties. The power conversion efficiency of the PSC based on **P3**:$PC_{70}BM$ = 1:1(w/w) reached 2.86% with short circuit current of 7.85 mA/cm^2, open circuit voltage of 0.68 V, and fill factor of 0.535, under the illumination of AM1.5, 100 mW/cm^2.

Introduction

In recent years, polymer solar cells (PSCs) have attracted considerable attention because of their advantages of low cost, easy fabrication, lightweight, and the capability to fabricate flexible large-area devices.[1−5] PSCs are composed of an active layer of the blend of a conjugated polymer donor and a fullerene derivative acceptor, sandwiched between an ITO positive electrode and a low workfunction metal negative electrode. Regioregular poly(3-hexylthiophene) (P3HT) and [6,6]-phenyl-C-61-butyric acid methyl ester (PCBM) are the most representative donor and acceptor materials respectively, and the power conversion efficiency (PCE) of the PSCs based on P3HT/PCBM have reached over 4%.[6] The advantage of P3HT is its higher hole mobility related to the appropriate aggregation of its simple 5-membered ring thiophene chain and regioregular alkyl side chain. But, the weak points of P3HT as the photovoltaic donor material are the mismatch of its absorption spectrum (absorption edge is at ca. 650 nm) with the solar spectrum and its high HOMO energy level (−4.76 eV)[7] which results in low open circuit voltage (ca. 0.6 V) of the PSCs with PCBM as acceptor. Obviously, broad absorption, higher hole mobility and lower laying HOMO energy level are very important for high efficiency conjugated polymer donor materials.

In order to improve the visible absorption and decrease HOMO energy level of the conjugated polymers, various narrow bandgap D−A copolymers of electron-rich (or donor, D) and electron-deficient (or acceptor, A) aromatic units were designed and synthesized in recent years.[8−20] Among the D−A copolymers, the copolymers of benzothiadiazole as the acceptor unit with fluorene or fluorene-like units (replacement of two benzene rings by two thiophene rings, or replacement of 9-C by Si or N) as the donor unit, show promising photovoltaic performance with the PCE values higher than 5%.[9a,12,13a] The D−A copolymers based on diketopyrrolopyrrole acceptor unit also attracted much interest recently.[16]

Thiazole is a well-known electron-deficient unit because it contains one electron-withdrawing nitrogen of imine (C=N) in place of the carbon atom at the 3-position of thiophene.[21−27] Bithiazole (BTz) with two thiazole rings connected together have also been used as acceptor unit to copolymerize with the donor unit of TF (PTHBTzTF),[28] oligothiophene unit with Pt in the polymer chain[29] or cyclopentadithiophene (CPDT),[30] and the PSCs based on the copolymers show high open circuit voltage and a PCE of around 3%.[29,30] These indicate that the copolymer-based BTz could also be promising photovoltaic donor materials. Obviously, BTz unit is simple in structure in comparison with other acceptor units such as benzothiadiazole etc. Nevertheless, only a limited number of BTz-based copolymers have been explored.

In this work, we synthesized three D−A alternative copolymers containing BTz acceptor unit and the donor unit of carbazole, dithienopyrrole or dithienosilole for searching new conjugated polymer photovoltaic donor materials. The three copolymers are poly{5,5′-bis(2-thienyl)-4,4,-dihexyl-2,2′-bithiazole-5′,5″-diyl-*alt*-N-9′-heptadecanyl-carbazole-2,7-diyl}(**P1**), poly{5,5′-Bis(2-thienyl)-4,4,-dihexyl-2,2′-bithiazole-5′,5″-diyl-*alt*-N-2-ethylhexyl-dithieno-[3,2-b:2′3′-d]-pyrrole-2,6-diyl} (**P2**), and poly{5,5′-bis(2-thienyl)-4,4,-dihexyl-2,2′-bithiazole-5′,5″-diyl-*alt*-4,4′- bis(2-ethylhexyl)-dithieno[3,2-b:2′,3′-d]-silole-5,5′-diyl}(**P3**), as shown in Scheme 2. Here we select three typical donor building blocks to tune the absorption and molecular energy levels to meet the requirements of a highly efficient photovoltaic polymer donor, and to investigate the relationships between their structures and properties, for the BTz-based copolymers.

Results and Discussion

Synthesis and Thermal Stability. The general synthetic strategy for monomer **2** and polymers is outlined in Schemes 1 and 2. The alternative copolymers of **P2** and **P3** were

*Corresponding authors. E-mail: (Y.L.) liyf@iccas.ac.cn.

 Published on Web 06/15/2010

synthesized by Stille coupling reaction, and **P1** was synthesized by Suzuki coupling reaction. All the polymers have good solubility in common organic solvents such as chloroform, toluene, and chlorobenzene. Molecular weights and polydispersity indices (PDIs) of the polymers, as shown in Table 1, are determined by gel permeation chromatography (GPC) analysis with a polystyrene standard calibration.

Thermal stability of the polymers was investigated with thermogravimetric analysis (TGA), as shown in Figure 1. The TGA analysis reveals that the onset temperatures with 5% weight-loss (T_d) of **P1**, **P2**, and **P3** are 257, 317, and 368 °C respectively. This indicates that the thermal stability of the copolymers is enough for the applications in optoelectronic devices.

Absorption Spectra. Figure 2 shows the ultraviolet−visible (UV−vis) absorption spectra of the polymer dilute solutions in chloroform and films spin-coated on quartz substrates. **P2** and **P3** solutions show similar absorption spectra with the absorption maxima at 513 and 510 nm (see Figure 2a), respectively. In comparison with the absorption spectra of **P2** and **P3** solutions, the **P1** solution shows a significantly

Table 1. Molecular Weights and Thermal Properties of the Polymers

polymers	M_w[a]	M_n[a]	PDI[a]	T_d (°C)[b]
P1	252.6K	73.7K	3.4	257
P2	9.3K	4.6K	1.78	317
P3	9.5K	5.6K	1.7	368

[a] M_n, M_w, and PDI of the polymers were determined by GPC using polystyrene standards in THF. [b] The 5% weight-loss temperatures under inert atmosphere.

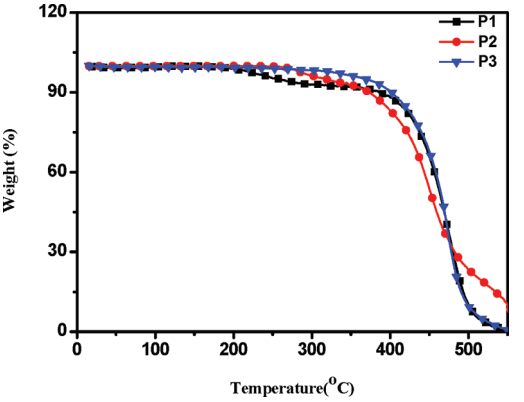

Figure 1. TGA plots of the copolymers with a heating rate of 10 °C/min under inert atmosphere.

Scheme 1. Synthetic Route for Monomer 2

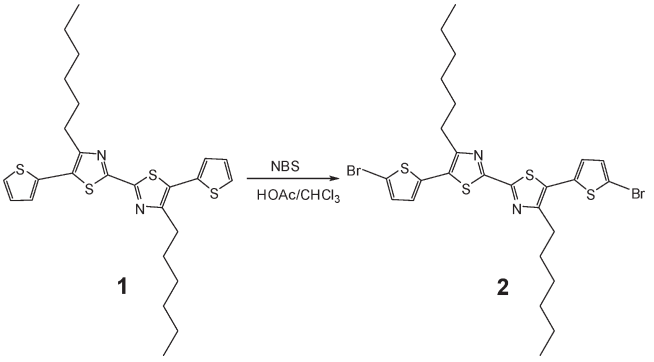

Scheme 2. Synthetic Route for the Copolymers

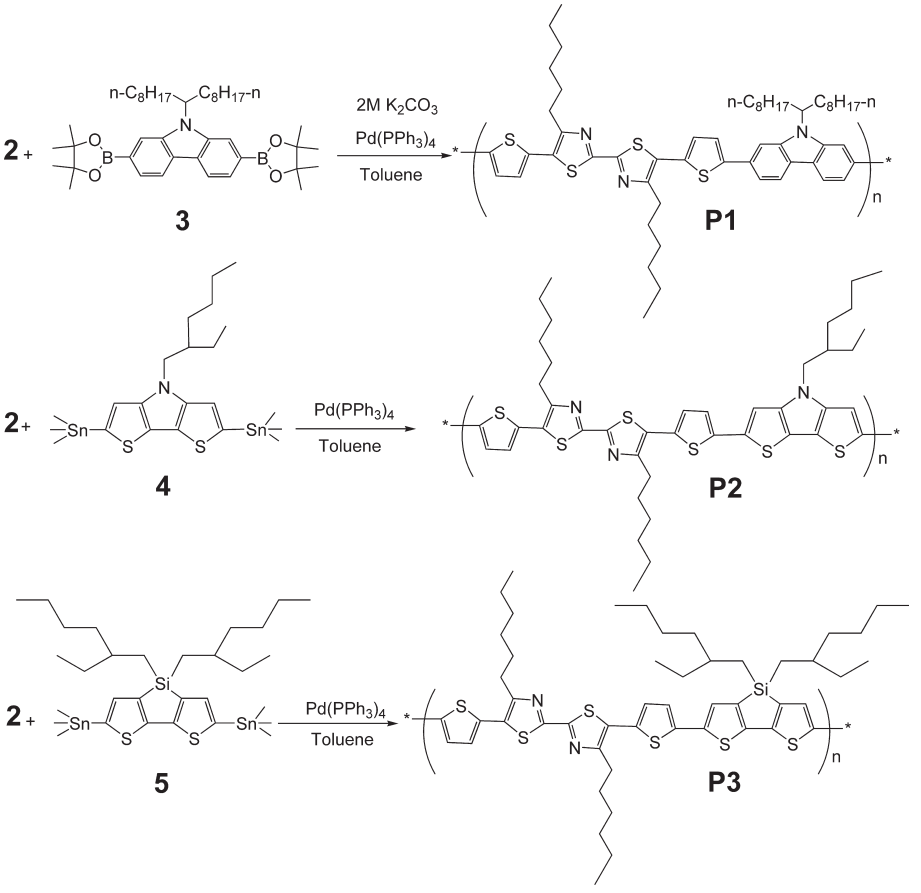

blue-shifted absorption band with an absorption peak at 463 nm. Figure 2b shows the absorbance of the polymer films for unit thickness. Among the three polymers, **P3** film displays strongest absorbance with the maximum of ca. 0.7×10^{-2}/nm at around 550 nm. Interestingly, the shape of the absorption peak of **P3** film is very similar to that of the regioregular P3HT film,[31] but the absorbance of **P3** film is weaker than that of P3HT film (the maximum absorbance of P3HT film is ca. 1.1×10^{-2}/nm at around 550 nm.[7]). The absorption spectra of the polymer films all show red-shift in comparison with that of their solutions, which is a common phenomenon for the conjugated polymers owing to the aggregation of the conjugated polymer main chains in the solid films. The detailed absorption data, including absorption maximum wavelength of solutions and films, the absorption edge (onset wavelength of the absorption peak, λ_{onset}) of the polymer films and the optical bandgap deduced from the absorption edges, are summarized in Table 2. Among the three polymers, the red-shift of the film absorption peak than its solution is the biggest for **P3**, the absorption maximum from 511 nm for **P3** solution to 558 nm for **P3** film, red-shifted by 48 nm. The absorption maximum of **P2** film is also red-shifted by 30 nm compared with that of its solution. The results indicate that there are strong intermolecular interactions in the **P2** and **P3** films. However, there is only 7 nm red-shift for **P1** from the solution to the film, due probably to the larger steric hindrance of the bulky heptadecanyl side chains in **P1** than that of 2-ethylhexyl side chain in **P2**. The absorption edges (λ_{edge}) of the three polymer films are 560 nm for **P1**, 740 nm for **P2**, and 670 nm for **P3**, from which the optical bandgaps (E_g^{opt}) of the polymers can be calculated according to $E_g^{opt} = 1240/\lambda_{edge}$. The E_g^{opt} values of **P1**, **P2**, and **P3** are 2.21, 1.68, and 1.85 eV respectively. These results suggest that by changing the donor segments with different electron-donating ability, the absorption spectra and bandgaps of the D−A copolymers can be tuned, which is very useful for the design of the photovoltaic materials.

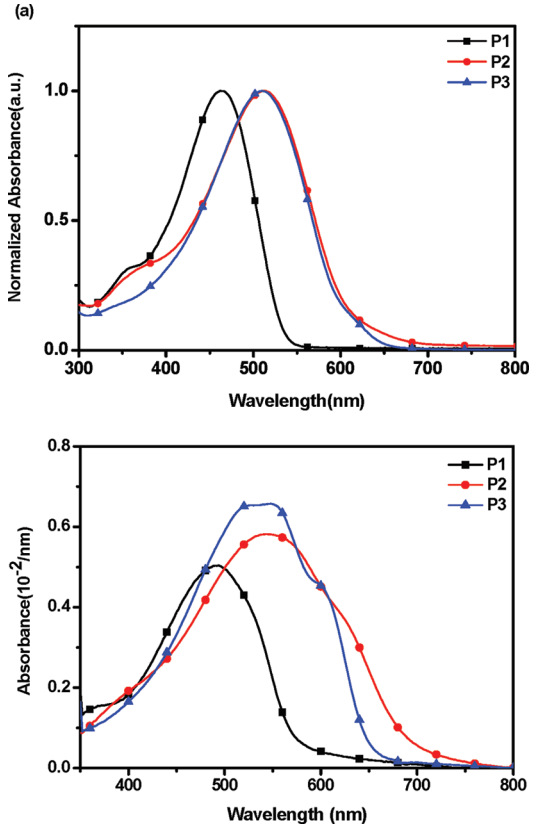

Figure 2. Absorption spectra of the copolymers (a) in chloroform solutions and (b) in solid films.

DSC and X-ray Diffraction. In order to investigate possible crystallization in the **P3** film in considering its similar absorption with P3HT, the differential scanning calorimetry (DSC) was measured. As shown in Figure 3, there is a weak endothermic peak at 243 °C, indicating that there is some local crystallization in **P3** film. The DSC was also measured for **P1** and **P2**, there are no peaks in the temperature range from room temperature to 280 °C.

Figure 4 shows the X-ray diffraction (XRD) patterns of the copolymers **P1**−**P3**. It is clear that there is no apparent peak at small angel region for all the three polymers, but they all have a broad peak centered at $2\theta = 24-25°$. The d spacing corresponding to the wide angel XRD peaks is 3.65, 3.49, and 3.52 Å for copolymers **P1**, **P2**, and **P3**, respectively, which are somewhat smaller than that (ca. 3.80 Å) observed in HT-P3AT.[32] The broad XRD peak indicates that the face-to-face stacking in the polymers occurs only in very small regions, and the copolymers mainly show amorphous structure.

Electrochemical Properties. The electrochemical cyclic voltammetry was performed for determining the highest occupied molecular orbital (HOMO) and the lowest unoccupied

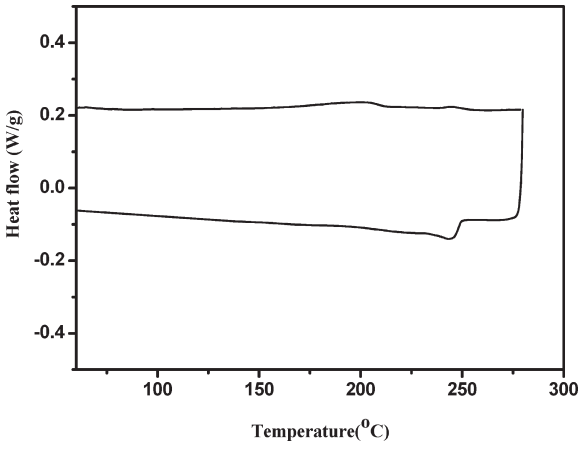

Figure 3. Differential scanning calorimetry of copolymer **P3**.

Table 2. Optical and Electrochemical Properties of the Polymers

	UV−vis absorption spectra				cyclic voltammetry		
	solution[a]	film[b]			p-doping	n-doping	
polymers	λ_{max} (nm)	λ_{max} (nm)	λ_{onset} (nm)	E_g^{opt} (eV)[c]	φ_{ox}/HOMO (V)/(eV)	φ_{red} /LUMO (V)/(eV)	E_g^{EC} (eV)
P1	464	472	540	2.21	0.73/−5.44	−1.80/−2.91	2.53
P2	509	540	750	1.68	0.05/−4.76	−1.92/−2.79	1.97
P3	511	558	670	1.85	0.47/−5.18	−1.62/−3.09	2.09

[a] Measured in chloroform solution. [b] Cast from chloroform solution. [c] Bandgap estimated from the onset wavelength (λ_{edge}) of the optical absorption: $E_g^{opt} = 1240/\lambda_{edge}$.

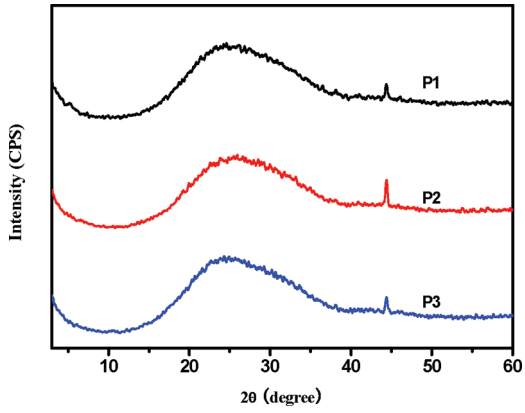

Figure 4. X-ray diffraction patterns of copolymers **P1**−**P3** films.

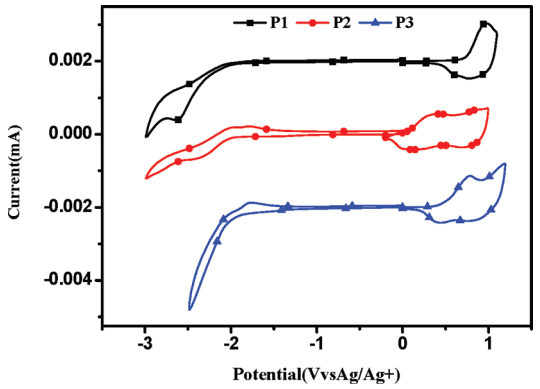

Figure 5. Cyclic voltammograms of **P1**, **P2**, and **P3** films on a platinum electrode measured in 0.1 mol/L Bu_4NPF_6 acetonitrile solutions at a scan rate of 100 mV/s.

molecular orbital (LUMO) energy levels of the conjugated polymers.[33] Figure 5 shows the cyclic voltammograms (CVs) of the **P1**, **P2**, and **P3** films on Pt disk electrode in 0.1 mol/L Bu_4NPF_6 acetonitrile solution. The onset reduction potentials (φ_{red}) of **P1**, **P2**, and **P3** are −1.80, −1.92, and −1.62 V vs. Ag/Ag^+, respectively, while the onset oxidation potentials (φ_{ox}) are 0.73, 0.05, and 0.47 V vs. Ag/Ag^+, respectively. From the onset oxidation potentials (φ_{ox}) and the onset reduction potentials (φ_{red}) of the polymers, HOMO and LUMO energy levels as well as the energy gap (E_g^{EC}) of the polymers were calculated according to the equations[34]

$$\text{HOMO} = -\text{e}(\varphi_{ox} + 4.71)\ (\text{eV})$$

$$\text{LUMO} = -\text{e}(\varphi_{red} + 4.71)\ (\text{eV})$$

$$Eg^{EC} = \text{e}(\varphi_{ox} - \varphi_{red})\ (\text{eV})$$

where the units of φ_{ox} and φ_{red} are V vs Ag/Ag^+.

The results of the electrochemical measurements are listed in Table 2. The LUMO energy levels of **P1**, **P2**, and **P3** are −2.91, −2.79, and −3.09 eV respectively. And the HOMO energy levels of **P1**, **P2**, and **P3** are −5.44, −4.76 and −5.18 eV, respectively. The electrochemical bandgaps are 2.53, 1.97, and 2.09 eV for **P1**, **P2**, and **P3**, respectively. Obviously, the incorporation of the more electron-rich dithienopyrrole unit in **P2** results in too high an HOMO energy level, which will lead to lower open circuit voltage (V_{oc}) of the PSCs based on **P2**, since V_{oc} of polymer solar cells is related to the difference

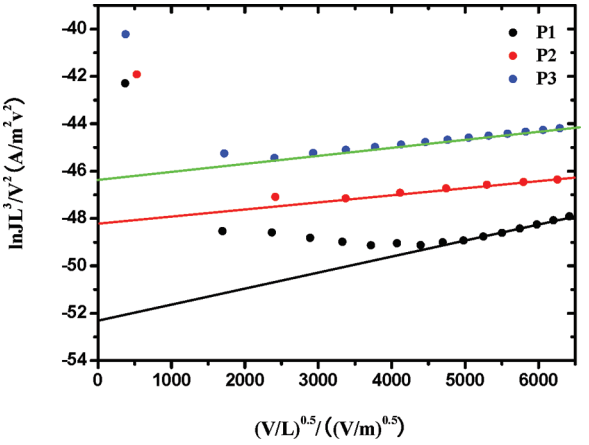

Figure 6. $\ln(JL^3/V^2)$ versus $(V/L)^{0.5}$ plots of the polymers for the measurement of hole mobility by the SCLC method.

of the LUMO of the electron acceptor and the HOMO of the electron donor.[35] The HOMO level of −5.18 eV for **P3** with dithienosilole group in its main chain is a suitable value for higher V_{oc} of the PSCs with the polymer as donor and PCBM as acceptor.

Hole Mobility. Hole mobility is another important parameter for the conjugated polymer donor photovoltaic materials. Here we measured the hole mobility of the copolymers **P1**−**P3** by space-charge limit current (SCLC) method by using a device structure of ITO/PEDOT:PSS/polymer/Au. For the hole-only devices, SCLC is described by

$$J \cong (9/8)\varepsilon\varepsilon_0\mu_0 V^2 \exp(0.89\sqrt{V/E_0 L})/L^3 \qquad (1)$$

where ε is the dielectric constant of the polymer, ε_0 is the permittivity of the vacuum, μ_0 is the zero-field mobility, E_0 is the characteristic field, J is the current density, L is the thickness of the blended films layer, $V = V_{appl} - V_{bi}$, V_{appl} is the applied potential, and V_{bi} is the built-in potential which results from the difference in the work function of the anode and the cathode (in this device structure, $V_{bi} = 0.2$ V). The results are plotted as $\ln(JL^3/V^2)$ versus $(V/L)^{0.5}$ (as shown in Figure 6). According to eq 1 and Figure 6, the hole mobilities obtained are 1.02×10^{-6}, 5.01×10^{-5}, and 3.07×10^{-4} cm^2/V s for **P1**, **P2**, and **P3**, respectively. Obviously, the hole mobility of **P3** is good for the application as photovoltaic donor materials in PSCs. However, the hole mobility of **P3** is lower than that ($> 10^{-3}$ cm^2/V s) of P3HT, due probably to the poorer packing structure in P3 in comparison with the highly ordered structure in P3HT.[32]

Photovoltaic Properties. To investigate and compare the photovoltaic properties of the three copolymers, bulk heterojunction PSC devices with a configuration of ITO/PEDOT:PSS/**P1**-**P3**:$PC_{60}BM$ (1:1 w/w)/Al were fabricated. Figure 7 shows the $I-V$ curves of the PSCs under the illumination of AM1.5, 100 mW/cm^2. The corresponding open-circuit voltage (V_{oc}), short-circuit current (I_{sc}), fill factor (FF), and power conversion efficiency (PCE) of the devices are summarized in Table 3. The PSCs based on **P1** and **P3** show higher V_{oc} of 0.82 and 0.70 V respectively, benefitted from lower HOMO energy levels of the two polymers. While the V_{oc} of the PSC based on **P2** is only 0.28 V, suffered from the too high HOMO energy level of the polymer. Among the PSCs, the device based on **P3**:$PC_{60}BM$ (1:1 w/w) displayed the best photovoltaic performance: PCE of 1.63% with a V_{oc} of 0.70 V, an I_{sc} of 5.14 mA/cm^2, and a fill factor (FF) of 0.451. The greater short circuit current of

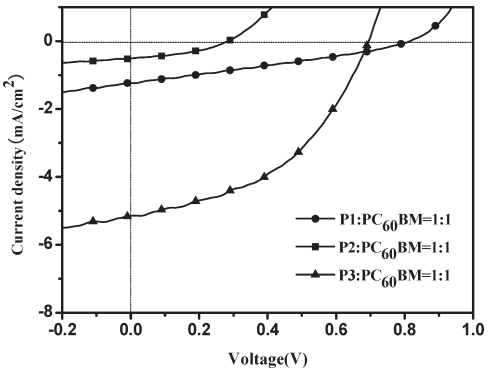

Figure 7. $I-V$ curves of the PSCs based on **P1**−**P3**:$PC_{60}BM$ (1:1, w/w), under the illumination of AM 1.5, 100 mW/cm^2.

Table 3. Photovoltaic Performances of the PSCs Based on P1−P3: $PC_{60}BM$ (1:1 w/w) under the Illumination of AM1.5, 100 mW/cm^2

polymer	V_{oc} (V)	I_{sc} (mA/cm^2)	FF	PCE (%)
P1	0.82	1.24	0.296	0.30
P2	0.28	0.51	0.337	0.06
P3	0.70	5.14	0.451	1.63

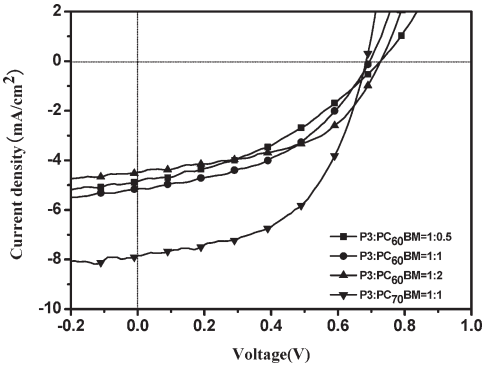

Figure 8. $I-V$ curves of the PSCs based on **P3**:$PC_{60}BM$ (or $PC_{70}BM$) with different weight ratios under the illumination of AM 1.5, 100 mW/cm^2.

Table 4. Photovoltaic Properties of the PSCs Based on P3 with Different Fullerene Acceptors and Different Weight Ratios, under the Illumination of AM1.5, 100 mW/cm^2

active layer	V_{oc}(V)	I_{sc}(mA/cm^2)	FF	PCE (%)
P3:$PC_{60}BM$ = 1:0.5	0.78	4.85	0.385	1.36
P3:$PC_{60}BM$ = 1:1	0.70	5.14	0.451	1.63
P3:$PC_{60}BM$ = 1:2	0.73	4.49	0.507	1.66
P3:$PC_{70}BM$ = 1:1	0.68	7.85	0.535	2.86

the device based on **P3** agrees with the stronger absorbance and higher hole mobility of **P3** film mentioned above.

In considering the promising photovoltaic properties of **P3** among the three copolymers, we performed the optimization on the PSCs based on **P3** by changing weight ratios of **P3**:$PC_{60}BM$ and by using $PC_{70}BM$ as acceptor instead of $PC_{60}BM$. Figure 8 shows the current−voltage characteristics of the PSC devices at different device fabrication conditions and Table 4 lists the photovoltaic properties of the devices. For the effect of the weight ratio of **P3**:$PC_{60}BM$ on the photovoltaic properties, in comparison with the PSC based on **P3**:$PC_{60}BM$ = 1:1, lower $PC_{60}BM$ weight ratio at **P3**:$PC_{60}BM$ = 1:0.5 led to lower I_{sc} (4.85 mA/cm^2) and lower PCE (1.36%) values (although its V_{oc} of 0.78 V is slightly higher), due probably to the inefficient charge separation

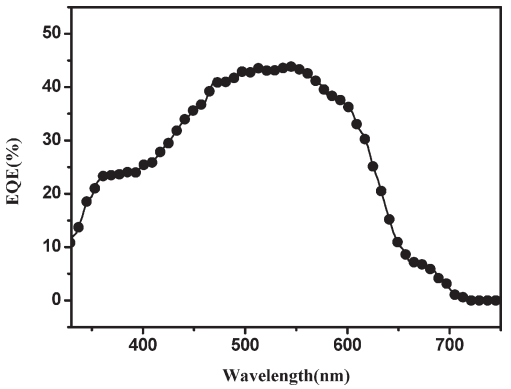

Figure 9. EQE of PSC based on **P3**:$PC_{70}BM$ (1:1 w/w).

and lower electron transporting efficiency.[36] While higher $PC_{60}BM$ weight ratio at **P3**:$PC_{60}BM$ = 1:2 w/w shows different effect on the photovoltaic properties: lower I_{sc} (4.49 mA/cm^2), slightly higher V_{oc} (0.73 V) and higher FF (0.507), resulting in a little higher PCE (1.66%). The lower I_{sc} at higher $PC_{60}BM$ content could be ascribed to the reduction of the absorption of the active layer and an unbalanced charge transporting properties between holes and electrons due to the high $PC_{60}BM$ content.[37]

For the effect of fullerene acceptors, $PC_{70}BM$ shows superior photovoltaic properties over $PC_{60}BM$ in the blend system with **P3**. The PCE of the PSC based on **P3**:$PC_{70}BM$ (1:1, w/w) reached 2.86% with V_{oc} = 0.68 V, I_{sc} = 7.85 mA/cm^2, and FF = 0.535 under the illumination of AM1.5, 100 mW/cm^2. Obviously, I_{sc} increased significantly by using $PC_{70}BM$ as acceptor, which could benefit from the enhanced visible absorption by $PC_{70}BM$ compared to $PC_{60}BM$. As shown in Figure 9, the EQE curve of the PSC based on **P3**:$PC_{70}BM$ covers a broad wavelength range from 350 to 700 nm with the maximum EQE value of 45% at ca. 550 nm.

Conclusion

We have successfully sythesized a series of donor−acceptor (D−A) copolymers containing bithiazole acceptor unit and different donor units, including **P1** with carbazole unit, **P2** with dithienopyrrole unit and **P3** with dithienosilole unit in their main chain, by the Pd-catalyzed Stille-coupling or Suzuki method. All the polymers exhibit good thermal stability. But, the donor units influence the absorption spectra, electronic energy levels and photovoltaic properties of the copolymers significantly. Among the three copolymers, **P3** film with the donor unit of dithienosilole shows stronger absorbance (ca. 0.7 × 10^{-2}/nm at around 550 nm) with an absorption spectrum similar to that of P3HT, lower HOMO energy level at −5.18 eV, higher hole mobility of 3.07 × 10^{-4} cm^2/V s and promising photovoltaic properties. The PCE of the PSC based on **P3**:$PC_{70}BM$ = 1:1(w/w) reached 2.86% with I_{sc} = 7.85 mA/cm^2, V_{oc} = 0.68 V, and FF = 0.535, under the illumination of AM1.5, 100 mW/cm^2. These results indicate that bithiazole is an effective acceptor segment for the design of D−A type photovoltaic conjugated polymers donor materials.

Experimental Section

Materials. All chemicals and solvents were reagent grades and purchased from Aldrich, Alfa Aesar and TCI Chemical Co, respectively. Toluene, tetrahydrofuran, and diethyl ether were distilled to keep anhydrous before use. The other solvents were degassed by nitrogen 1 h prior to use, unless otherwise stated.

Measurements and Characterization. All new compounds were characterized by ^{1}H NMR spectroscopy performed on a

Bruker DMX-400 spectrometer. For the ^{1}H NMR measurements, $CDCl_3$ was used as the solvent. Chemical shifts in the NMR spectra were reported in ppm relative to the singlet at 7.26 ppm for $CDCl_3$. The molecular weight of the polymers was measured by gel permeation chromatography (GPC), and polystyrene was used as a standard. Thermogravimetric analysis (TGA) was performed on a Perkin−Elmer TGA-7. Mass spectra were obtained with a Shimadzu QP2010 spectrometer. UV−vis absorption spectra were obtained on a Hitachi U-3010 spectrometer. Fluorescence spectra were obtained on a Hitachi F-4500 spectrometer. Cyclic voltammetry (CV) was performed on a Zahner IM6e electrochemical workstation with a three-electrode system in a solution of 0.1 M Bu_4NPF_6 in acetonitrile at a scan rate of 100 mV/s. The polymer films were coated on a Pt plate electrode (1.0 cm^2) by dipping the electrode into the corresponding solutions and then drying. A Pt wire was used as the counter electrode, and Ag/Ag^+ was used as the reference electrode.

Device Fabrication and Characterization of Polymer Solar Cells. Polymer solar cells (PSCs) were fabricated with ITO glass as a positive electrode, Ca/Al as a negative electrode and the blend film of the polymer/PCBM between them as a photosensitive layer. The ITO glass was precleaned and modified by a thin layer of PEDOT:PSS which was spin-cast from a PEDOT:PSS aqueous solution (Clevious P VP AI 4083 H. C. Stark, Germany) on the ITO substrate, and the thickness of the PEDOT: PSS layer is about 60 nm. The photosensitive layer was prepared by spin-coating a blend solution of polymers and $PC_{61}BM$ or $PC_{71}BM$ in o-dichlorobenzene on the ITO/PEDOT:PSS electrode. Then the Ca/Al cathode was deposited on the polymer layer by vacuum evaporation under 3×10^{-4} Pa. The thickness of the photosensitive layer is ca. 80 nm, measured on an Ambios Tech. XP-2 profilometer. The effective area of one cell is 4 mm^2. The current−voltage (*I-V*) measurement of the devices was conducted on a computer-controlled Keithley 236 Source Measure Unit. A xenon lamp with AM1.5 filter was used as the white light source, and the optical power at the sample was around 100 mW/cm^2.

Synthesis of Monomers. The following compounds were synthesized according to the procedure in the literature:,4,4′-dihexyl-5,5′-di(thiophen-2-yl)-2,2′-bithiazole(**1**),[29,30]2,7-bis(4′,4′,5′,5′-tetramethyl-1′,3′,2′-dioxaborolan-2′-yl)-*N*-9″-heptadecanylcarbazole (**3**),[10] *N*-2-ethylhexyl-2,6-bis(trimethylstannyl)dithieno-[3,2-*b*:2′3′-*d*]-pyrrole (**4**),[14] 4,4′-bis(2-ethylhexyl)-5,5′-bis(trimethyltin)dithieno[3,2-*b*:2′,3′-*d*]silole (**5**).[13] The synthetic routes of Monomer **2** and the copolymers are shown in Schemes 1 and 2. The detailed synthetic processes are as follows.

5,5′-Bis(5-bromo-2-thienyl)-4,4′-dihexyl-2,2′-bithiazole (*2*). Compound **1** (4 g, 8 mmol) was dissolved in a mixture of chloroform (40 mL) and glacial acetic acid (10 mL). NBS (2.92 g, 16.4 mmol) was then added to the solution and stirred for 1 h in the dark. The precipitate in the reaction mixture was filtered, washed with methanol, and then dried to produce the dibromo product **2** (3.7 g, yield = 70%). ^{1}H NMR (400 MHz, $CDCl_3$), δ (ppm): 7.03 (d, 2H), 6.92 (d, 2H), 2.86 (t, 4H), 1.72 (m, 4H), 1.40−1.15 (m, 12H), 0.87 (t, 6H). MS: m/z = 656.

Synthesis of BT-Containing D−A Copolymers. *Poly{5,5′-Bis(2-thienyl)-4,4′-dihexyl-2,2′-bithiazole-5′,5″-diyl-alt-N-9′-heptadecanylcarbazole-2,7-diyl}* (***P1***). Monomer **2** (656 mg, 1.0 mmol), monomer **3** (657 mg, 1.0 mmol), Pd $(PPh_3)_4$ (0.023 g, 0.020 mmol), and phase-transfer catalyst Aliquat 336 (40 mg, 0.10 mmol were dissolved in toluene (6 mL). 2.3 mL aqueous solution of sodium carbonate (2 mol/L) was then added to the reaction mixture. The polymerization was carried out at 90 °C for 2 days and was end-capped with bromobenzene and phenylboronic acid. The mixture was allowed to reflux for 2 h and cooled to room temperature, and the polymer was precipitated by slowly adding the mixture into CH_3OH. The precipitates were collected by filtration and then washed with MeOH and hexane. The solid was dissolved in $CHCl_3$ (150 mL) and passed through a column packed with alumina, Celite, and silica gel. The column was eluted with $CHCl_3$. The combined polymer solution was concentrated and was poured into MeOH. After this, the precipitates were collected and dried under vacuum overnight to get **P1**. Yield: 600 mg (67%). GPC: M_w = 252.6K; M_n = 73.7K; M_w/M_n = 3.4. ^{1}H NMR (400 MHz, $CDCl_3$), δ (ppm): 8.1 (s, 2H), 7.88−7.35 (m, 8H), 4.60 (s, 1H), 3.06 (s, 4H), 2.10−1.75 (m, 4H), 1.57−1.03 (m, 40H), 0.99−0.73 (m, 12H).

Poly{5,5′-Bis(2-thienyl)-4,4′-dihexyl-2,2′-bithiazole-5′,5″-diyl-alt-N-2-ethylhexyldithieno[3,2-b:2′3′-d]-pyrrole-2,6-diyl} (***P2***). Monomer **2** (328 mg, 0.5 mmol), monomer **4** (309 mg, 0.5 mmol), and dry toluene (15 mL) were added to a 50 mL double-neck round-bottom flask. The reaction container was purged with N_2 for 20 min to remove O_2, and then Pd $(PPh_3)_4$ (15 mg, 0.013 mmol) was added. After another flushing with N_2 for 20 min, the reactant was heated to reflux for 8 h. The reactant was cooled down to room temperature and poured into MeOH (200 mL), and the precipitates were collected by filtration and then washed with MeOH. The solid was dissolved in $CHCl_3$ (100 mL) and passed through a column packed with alumina, Celite, and silica gel. The column was eluted with $CHCl_3$. The combined polymer solution was concentrated and was poured into MeOH. After this, the precipitates were collected and dried under vacuum overnight to get **P2**. Yield: 184 mg (47%). GPC: M_w = 9.3K; M_n = 4.6K; M_w/M_n = 1.78. ^{1}H NMR (400 MHz, $CDCl_3$), δ (ppm): 7.32−7.22 (m, 6H), 4.02 (s, 2H), 2.99 (s, 5H), 1.85 (m, 8H), 1.55−1.40 (m, 16H), 1.0−0.79 (m, 12H).

Poly{5,5′-Bis(2-thienyl)-4,4′-dihexyl-2,2′-bithiazole-5′,5″-diyl-alt-4,4′-Bis(2-ethylhexyl)dithieno[3,2-b:2′,3′-d]-silole-5,5′-diyl} (***P3***). The polymerization process was the same as that for P2, except that monomer **5** was used instead of monomer **4** and the reactant was refluxed for 18 h. Yield: 227 mg (50%). GPC: M_w = 9.5K; M_n = 5.6K; M_w/M_n = 1.7. ^{1}H NMR (400 MHz, $CDCl_3$), δ (ppm): 7.16−7.05 (m, 6H), 2.99 (s, 4H), 1.85 (m, 8H), 1.55−1.40 (m, 12H), 1.2−1.03 (m, 18H), 0.87−0.64 (m, 18H).

Acknowledgment. This work was supported by the NSFC (Nos. 50633050, 20721061, 20821120293, and 50933003), and Chinese Academy of Sciences.

References and Notes

(1) Yu, G.; Gao, J.; Hummelen, J. C.; Wudl, F.; Heeger, A. J. *Science* **1995**, *270*, 1789–1791.
(2) Chen, H.-Y.; Hou, J. H.; Zhang, S. Q.; Liang, Y. Y.; Yang, G. W.; Yang, Y.; Yu, L. P.; Wu, Y.; Li, G. *Nat. Photonics* **2009**, *3*, 649–653.
(3) (a) Chen, J. W.; Cao, Y. *Acc. Chem. Res.* **2009**, *42*, 1709–1718. (b) Li, Y. F.; Zou, Y. P. *Adv. Mater.* **2008**, *20*, 2952–2958.
(4) Thompson, B. C.; Fréchet, J. M. J. *Angew. Chem., Int. Ed.* **2008**, *47*, 58–77.
(5) Park, S. H.; Roy, A.; Beaupré, S.; Cho, S.; Coates, N.; Moon, J. S.; Moses, D.; Leclerc, M.; Lee, K. H.; Heeger, A. J. *Nat. Photonics* **2009**, *3*, 297–303.
(6) (a) Li, G.; Shrotriva, V.; Huang, J. S.; Yao, Y.; Moriarty, T.; Emery, K.; Yang, Y. *Nat. Mater.* **2005**, *4*, 864–868. (b) Ma, W. L.; Yang, C. Y.; Gong, X.; Lee, K.; Heeger, A. J. *Adv. Funct. Mater.* **2005**, *15*, 1617–1622.
(7) Hou, J. H.; Tan, Z. A.; Yan, Y.; He, Y. J.; Yang, C. H.; Li, Y. F. *J. Am. Chem. Soc.* **2006**, *128*, 4911.
(8) (a) Muhlbacher, D.; Scharber, M.; Morana, M.; Zhu, Z. G.; Waller, D.; Gaudiana, R.; Brabec, C. *Adv. Mater.* **2006**, *18*, 2884. (b) Zhu, Z.; Waller, D.; Gaudiana, R.; Morana, M.; Muhlbacher, D.; Scharber, M.; Brabec, C. *Macromolecules* **2007**, *40*, 1981–1986. (c) Svensson, M.; Zhang, F. L.; Veenstra, S. C.; Verhees, W. J. H.; Hummelen, J. C.; Kroon, J. M.; Inganas, O.; Andersson, M. R. *Adv. Mater.* **2003**, *15*, 988.
(9) (a) Zhou, Q. M.; Hou, Q.; Zheng, L. P.; Deng, X. Y.; Yu, G.; Cao, Y. *Appl. Phys. Lett.* **2004**, *84*, 1653–1655. (b) Yang, R. Q.; Tian, R. Y.; Yan, J. G.; Zhang, Y.; Yang, J.; Hou, Q.; Yang, W.; Zhang, C.; Cao, Y. *Macromolecules* **2005**, *38*, 244–253. (c) Xia, Y. J.; Deng, X. Y.; Wang, L.; Li, X. Z.; Zhu, X. H.; Cao, Y. *Macromol. Rapid Commun.* **2006**, *27*, 1260–1264.

(10) (a) Blouin, N.; Michaud, A.; Leclerc, M. *Adv. Mater*. **2007**, *19*, 2295. (b) Blouin, N.; Michaud, A.; Gendron, D.; Wakim, S.; Blair, E.; Neagu-Plesu, R.; Belletete, M.; Durocher, G.; Tao, Y.; Leclerc, M. *J. Am. Chem. Soc*. **2008**, *130*, 732–742.
(11) Huo, L. J.; He, C.; Han, M. F.; Zhou, E. J.; Li, Y. F. *J. Polym. Sci. A: Polym. Chem*. **2007**, *45*, 3861–3871.
(12) Peet, J.; Kim, J. Y.; Coates, N. E.; Ma, W. L.; Moses, D.; Heeger, A. J.; Bazan, G. C. *Nat. Mater*. **2007**, *6*, 497–500.
(13) (a) Hou, J. H.; Chen, H. Y.; Zhang, S. Q.; Li, G.; Yang, Y. *J. Am. Chem. Soc*. **2008**, *130*, 16144. (b) Hou, J. H.; Chen, H. Y.; Zhang, S. Q.; Yang, Y. *J. Phys. Chem. C* **2009**, *113*, 21202–21207.
(14) (a) Zhou, E. J.; Nakamura, M.; Nishizawa, T.; Zhang, Y.; Wei, Q. S.; Tajima, K.; Yang, C. H.; Hashimoto, K. *Macromolecules* **2008**, *41*, 8302–8305. (b) Zhou, E. J.; Yamakawa, S.; Zhang, Y.; Tajima, K.; Yang, C. H.; Hashimoto, K. *J. Mater. Chem*. **2009**, *19*, 7730–7737. (c) Zhou, E. J.; Yamakawa, S. P.; Tajima, K.; Yang, C. H.; Hashimoto, K. *Chem. Mater*. **2009**, *21*, 4055–4061.
(15) Yue, W.; Zhao, Y.; Shao, S. Y.; Tian, H. K.; Xie, Z. Y.; Geng, Y. H.; Wang, F. S. *J. Mater. Chem*. **2009**, *19*, 2199–2206.
(16) (a) Zou, Y. P.; Gendron, D.; Badrou-Aich, R.; Najari, A.; Tao, Y.; Leclerc, M. *Macromolecules* **2009**, *42*, 2891–2894. (b) Zou, Y. P.; Gendron, D.; Neagu-Plesu, R.; Leclerc, M. *Macromolecules* **2009**, *42*, 6361–6365.
(17) Zhan, X. W.; Tan, Z. A.; Domercq, B.; An, Z. S.; Zhang, X.; Barlow, S.; Li, Y. F.; Zhu, D. B.; Kippelen, B.; Marder, S. R. *J. Am. Chem. Soc*. **2007**, *129*, 7246–7247.
(18) Lee, S. K.; Cho, N. S.; Kwak, J. H.; Lim, K. S.; Shim, H. K.; Hwang, D. H.; Brabec, C. J. *Thin Solid Films* **2006**, *511*, 157–162.
(19) Thompson, B. C.; Kim, Y. G.; McCarley, T. D.; Reynolds, J. R. *J. Am. Chem. Soc*. **2006**, *128*, 12714–12725.
(20) Colladet, K.; Fourier, S.; Cleij, T. J.; Lutsen, L.; Gelan, J.; Vanderzande, D.; Nguyen, L. H.; Neugebauer, H.; Sariciftci, S.; Aguirre, A.; Janssen, G.; Goovaerts, E. *Macromolecules* **2007**, *40*, 65–72.
(21) (a) Yamamoto, T.; Suganuma, H.; Maruyama, T.; Inoue, T.; Muramatsu, Y.; Arai, M.; Komarudin, D.; Ooba, N.; Tomaru, S.; Sasaki, S.; Kubota, K. *Chem. Mater*. **1997**, *9*, 1217–1225. (b) Yamamoto, T.; Arai, M.; Kokubo, H.; Sasaki, S. *Macromolecules* **2003**, *36*, 7986–7993. (c) Yasuda, T.; Sakai, Y.; Aramaki, S.; Yamamoto, T. *Chem. Mater*. **2005**, *17*, 6060–6068.
(22) Politis, J. K.; Curtis, M. D.; Gonzalez, L.; Martin, D. C.; He, Y.; Kanicki, J. *Chem. Mater*. **1998**, *10*, 1713–1719.
(23) (a) Cao, J.; Curtis, M. D. *Chem. Mater*. **2003**, *15*, 4424–4430. (b) Cao, J.; Kampf, J. W.; Curtis, M. D. *Chem. Mater*. **2003**, *15*, 404–411.
(24) Yamamoto, T.; Otsuka, S.; Namekawa, K.; Fukumoto, H.; Yamaguchi, I.; Fukuda, T.; Asakawa, N.; Yamanobe, T.; Shiono, T.; Cai, Z. G. *Polymer* **2006**, *47*, 6038–6041.
(25) Mamada, M.; Nishida, J. I.; Kumaki, D.; Tokito, S.; Yamashita, Y. *Chem. Mater*. **2007**, *19*, 5404–5409.
(26) Sauve, G.; McCullough, R. D. *Adv. Mater*. **2007**, *19*, 1822.
(27) Naraso; Wudl, F. *Macromolecules* **2008**, *41*, 3169–3174.
(28) Lee, J.; Jung, B. J.; Lee, S. K.; Lee, J. I.; Cho, H. J.; Shim, H. K. *J. Polym. Sci. A Polym. Chem*. **2005**, *43*, 1845–1857.
(29) Wong, W. Y.; Wang, X. Z.; He, Z.; Chan, K. K.; Djurisic, A. B.; Cheung, K. Y.; Yip, C. T.; Ng, A. M. C.; Xi, Y. Y.; Mak, C. S. K.; Chan, W. K. *J. Am. Chem. Soc*. **2007**, *129*, 14372–14380.
(30) Li, K. C.; Huang, J. H.; Hsu, Y. C.; Huang, P. J.; Chu, C. W.; Lin, J. T.; Ho, K. C.; Wei, K. H.; Lin, H. C. *Macromolecules* **2009**, *42*, 3681–3693.
(31) Yang, C.; Orfino, F. P.; Holdcroft., S. *Macromolecules* **1996**, *29*, 6510–6517.
(32) McCullough, R. D.; Tristram-Nagle, S.; Williams, S. P.; Lowevt, R. D.; Jayaraman., M. *J. Am. Chem. Soc*. **1993**, *115*, 4910–4911.
(33) Li, Y. F.; Cao, Y.; Gao, J.; Wang, D. L.; Yu, G.; Heeger, A. J. *Synth. Met*. **1999**, *99*, 243–248.
(34) Sun, Q. J.; Wang, H. Q.; Yang, C. H.; Li, Y. F. *J. Mater. Chem*. **2003**, *13*, 800–806.
(35) Scharber, M. C.; Mühlbacher, D.; Koppe, M.; Denk, P.; Waldauf, C.; Heeger, A. J.; Brabec, C. J. *Adv. Mater*. **2006**, *18*, 789.
(36) (a) Quist, P. A. C.; Savenije, T. J.; Koetse, M. M.; Veenstra, S. C.; Kroon, J. M.; Siebbeles, L. D. A. *Adv. Funct. Mater*. **2005**, *15*, 469–474. (b) Baek, N. S.; Hau, S. K.; Yip, H. L.; Acton, O.; Chen, K. S.; Jen, A. K. Y. *Chem. Mater*. **2008**, *20*, 5734–5736.
(37) Huang, J. H.; Ho, Z. Y.; Kekuda, D.; Chang, Y.; Chu, C. W.; Ho, K. C. *Nanotechnology* **2009**, *20*, 025202.